

# The Structural Stability of Seven-Coordinate Divalent Cations in the First Transition Series Relevant to the Water-Exchange Reaction Mechanism

Yuko Tsutsui, Hiroaki Wasada,<sup>\*,†</sup> and Shigenobu Funahashi

Laboratory of Analytical Chemistry, Faculty of Science, Nagoya University, Nagoya 464-8602

<sup>†</sup>Faculty of Regional Studies, Gifu University, Gifu 501-1193

(Received January 12, 1998)

We studied the structural stability of heptahydrated divalent cations in the first transition series as model intermediary species in associative reaction pathways for the water exchange of hexahydrated cations by ab initio molecular-orbital methods. All of the structures of *heptacoordination* are pentagonal bipyramidal with a distorted equatorial plane. The structural stabilities are strongly dependent on their *d*-electron configurations. An associative mechanism is possible for the water-exchange reactions of hexahydrated divalent cations having less than seven *d* electrons, because the seven-coordinate species are located at the local minima or at the saddle points on the potential-energy surface. The occupation of the antibonding *b* orbital induces a transition density corresponding to an antisymmetric distortion through an interaction with a low-lying 4*s* orbital. The large bonding interaction makes the heptahydrated manganese(II) ion to become located at a local minimum. The occupancy of antibonding *a* orbitals determines the pattern of the antibonding interaction. Hexahydrated divalent cations with *d*<sup>3</sup>, *d*<sup>6</sup>, and *d*<sup>7</sup> configurations (vanadium(II), iron(II), and cobalt(II)) prefer a *cis* attack, while chromium(II) with a *d*<sup>4</sup> configuration prefers a *trans* attack during the operative associative process of the water-exchange reaction.

A ligand-substitution reaction, which is the replacement of a coordinating ligand by an entering ligand, is one of the most important reactions, as well as the electron-transfer and isomerization reactions in coordination chemistry. The substitution mechanisms are classified as to the degree of bond making and breaking of the entering and leaving ligands, i.e., an associative (A) mechanism, an associative-interchange (I<sub>a</sub>) mechanism, a dissociative-interchange (I<sub>d</sub>) mechanism, and a dissociative (D) mechanism.<sup>1)</sup> There have been a number of studies concerning the reaction mechanisms of ligand-substitution reactions, while the stereochemistry of their reaction pathways has not yet been clarified.

An ion in solution is solvated by solvent molecules where coordinating solvent molecules are always replaced by bulk solvent molecules. This quite simple process, called a solvent-exchange reaction, is regarded as being one of the most fundamental reactions, due to symmetry. In an aqueous solution, divalent cations in the first transition series are hexahydrated.<sup>2)</sup> Many experimental studies performed on the basis of activation parameters, especially the activation volume, have suggested that the operative mechanism of the water-exchange reaction of octahedrally hexahydrated divalent cations varies from I<sub>a</sub> for earlier members to I<sub>d</sub> for later members in the first transition series.<sup>3)</sup>

Recently, the reaction mechanisms have been theoretically discussed in some investigations along with a characterization of the intermediary species on the reaction pathways. The energetical characteristic of the intermediary species is

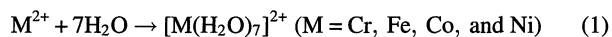
treated as a probe of the reaction mechanisms, for example, a correlation between the actual rate constants and the gas-phase dissociation energies of the expected intermediary species<sup>4a,4b)</sup> and a molecular orbital diagram between a reactant and an intermediary species.<sup>4c)</sup> Recent studies are also intended for structural characterizations as well as the stereochemistry of the intermediary species of the associative and the dissociative processes, i.e., intermediary species with seven water molecules in the first coordination shell (*heptacoordination*; [M(H<sub>2</sub>O)<sub>7</sub>]<sup>2+</sup>) and intermediary species with five water molecules in the first coordination shell and two water molecules in the second coordination shell (*pentacoordination*; [M(H<sub>2</sub>O)<sub>5</sub>]<sup>2+</sup>·2H<sub>2</sub>O), respectively.<sup>5,6)</sup> According to the results, the *pentacoordinations* are located at local minima for all members of the first transition series, while the structural stability of the *heptacoordinations*, which are intermediary species in the case of the associative mechanism, is remarkably dependent on the central cations. There is an overall decrease in the structural stability from the local minimum to the second-order saddle-point, corresponding to the change in the central cations from earlier members to later ones. The structural stability of *heptacoordination* determines the operative mechanisms of the water-exchange reactions; i.e., an associative mechanism is expected for the operative mechanism of only the earlier members, while the dissociative mechanism is feasible for all members in the first transition series. We have explained the dependency of the structural stability upon the occupancy

of the  $\sigma$ -antibonding  $d$  orbitals, and predicted the tendency of the structural stability of the earlier members in the first transition series.<sup>3)</sup> It is important to investigate the origin of the stabilization of seven-coordination, which is rarely found in complexes of the first transition series in contrast to that in commonly observed six-coordinate octahedral complexes.

In this paper, we concentrate on the heptahydrated divalent cations in the first transition series and investigate the origin of the structural stability from the viewpoint of electronic structure theory. Especially, we discuss the electronic effect based on the manner of distortion in unstable structures which determines the stereochemistry for the water-exchange reaction.

### Computational Details

We determined the structures of heptahydrated divalent cations ( $[M(H_2O)_7]^{2+}$ ;  $M = Fe, Co,$  and  $Ni$ ) and characterized their structural stability on the potential-energy surface by frequency calculations. The heptahydrated chromium(II) ion was reoptimized under a constraint of  $C_2$  symmetry for the convenience of analyzing the molecular orbitals. The hydration energies for reaction 1 were also calculated and compared with the structural stabilities.



All of the calculations were performed using a double-zeta plus polarization basis set. The [8s4p3d] segmented contraction of the (14s9p5d) primitive sets of Wachters was used for the central cations.<sup>7)</sup> The  $s$  and  $p$  spaces were contracted using contraction number 1, while the  $d$  space was contracted to [311]. We used the Huzinaga–Dunning [4s2p]/(9s5p) basis set for oxygen and [2s]/(4s) for hydrogen.<sup>8)</sup> The basis set of hydrogen was scaled by the factor of 1.2. Two  $4p$  functions of Wachters, scaled by the factor of 1.5, were added to the basis set of a central cation,<sup>7)</sup> one  $d$  polarization function was added to the basis set of oxygen ( $\alpha_O = 0.85$ ), and one  $p$  polarization function was added to the basis set of hydrogen ( $\alpha_H = 1.0$ ).

Previously, Åkesson et al. carried out CASSCF calculations with all five  $3d$  orbitals as the active space for hexahydrated titanium(II), iron(II), and cobalt(II) ions in order to examine the non-dynamical correlation effect for this type of open-shell system.<sup>9)</sup> They indicated, then, that the hydration energies given by CASSCF and SCF were not significantly different and that the mixing of states was merely an atomic effect. In the present work we examined the difference in the structures optimized by MP2 and SCF calculations for the heptahydrated iron(II), cobalt(II), and nickel(II) ions in the B states. We carried out geometry optimizations using the same basis set as described above, except for the polarization function of hydrogen ([8s6p3d] for metal, [4s2p1d] for oxygen, and [2s] for hydrogen) at the UHF and MP2 levels. All the optimized structures have  $C_2$  symmetry as shown in Fig. 1. The bond lengths (Å) of  $M-O_1$ ,  $M-O_2$ ,  $M-O_4$ , and  $M-O_6$  for the optimized structures at the MP2 level (in parentheses, the structural parameters at the UHF

level) are 2.259 (2.310), 2.288 (2.322), 2.293 (2.344), and 2.159 (2.196) for iron(II), 2.245 (2.302), 2.219 (2.263), 2.268 (2.315), and 2.147 (2.176) for cobalt(II), and 2.121 (2.148), 3.007 (3.083), 2.033 (2.069), and 2.057 (2.091) for nickel(II), respectively. The numbering of the oxygen atoms is defined in Fig. 1. The bond angles (degree) of  $\angle O_2MO_1$ ,  $\angle O_4MO_1$ , and  $\angle O_6MO_1$  in the optimized structures are 76.6 (77.1), 142.8 (143.5), and 82.3 (82.2) for iron(II), 78.6 (78.5), 142.3 (143.3), and 81.4 (81.2) for cobalt(II) and 69.3 (69.4), 131.1 (130.9), and 85.3 (85.7) for nickel(II), respectively. The difference in bond length between the two levels is less than 0.06 Å, except for the longest bond ( $M-O_2$ ) of the heptahydrated nickel(II) ion, while the order of the bond length is independent of the methodology. The difference in the bond angle is less than  $2^\circ$ , and that in the dihedral angle is less than  $3^\circ$ . The electron correlation estimated by a MP2 calculation indicates no significant effect on the pentagonal bipyramid with the distorted equatorial plane. The MP2 optimized structures were not significantly different from the SCF structures for earlier members.<sup>5b)</sup> Therefore, we carried out structural calculations at the UHF level. The basis set superposition errors (BSSE) involved in the hydration energies were estimated by the Boys–Bernardii counterpoise method.<sup>10)</sup>

We used the Gaussian92<sup>11a)</sup> and Gaussian94<sup>11b)</sup> programs on an IBM RS6000 for all ab initio molecular-orbital calculations and the MOLCAT program<sup>12a)</sup> on a Macintosh for visualizing the molecular structures and vibrational modes. We drew contour maps and three-dimensional structures of the molecular orbitals using the MOPLOT program<sup>12b)</sup> in order to interpret their spatial distribution. We denote energy in  $\text{kcal mol}^{-1}$  ( $1 \text{ kcal mol}^{-1} = 4.1884 \text{ kJ mol}^{-1}$ ) and in atomic unit (a.u.,  $1 \text{ a.u.} = 627.50959 \text{ kcal mol}^{-1}$ ) and bond length in Å ( $1 \text{ Å} = 100 \text{ pm}$ ).

### Results and Discussion

All of the structures of the *heptacoordinations* obtained in this study are pentagonal bipyramidal with a distorted equatorial plane. Figure 1 shows the structures of heptahydrated iron(II) and nickel(II) ions as two representative structures

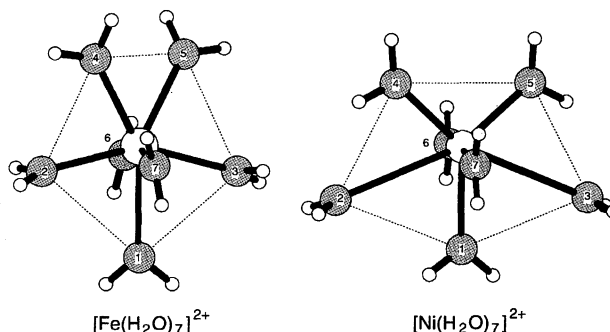


Fig. 1. The structures of heptahydrated iron(II) and nickel(II) ions. The numbering of oxygen atoms is shown. The atoms connected by dashed lines are placed on the equatorial plane of a pentagonal bipyramid.

of *heptacoordinations*, with numbering of the oxygen atoms. The equatorial plane of the heptahydrated nickel(II) ion is flatter than that of heptahydrated iron(II) ion. The dihedral angles of  $O_4-M-O_1-O_2$  are  $39.1^\circ$  for the iron(II) ion and  $0.0^\circ$  for the nickel(II) ion. The heptahydrated chromium(II) and nickel(II) ions have flatter equatorial planes. Tables 1 and 2 tabulate the structural parameters and electronic states for all of the heptahydrated divalent cations in the first transition series. The structural parameters for the optimized geometry of the heptahydrated cations are in good agreement with those obtained by previous studies.<sup>6)</sup> The heptahydrated cobalt(II) ion is located at the saddle point with a small negative curvature. Both of the  $^5A$  and  $^5B$  heptahydrated iron(II) ions are located at the saddle point, and the  $^5B$  state is lower in energy than the  $^5A$  state by  $0.4 \text{ kcal mol}^{-1}$ .

The imaginary modes of all of the *heptacoordinations* at the saddle points are shown in Fig. 2. They correspond to an antisymmetric stretching which follows a concerted motion of both the entering of a water molecule toward the central cation and the leaving of a water molecule on the opposite side of the  $C_2$  axis away from the central cation, and causes a distortion leading to the structure with six water molecules in the first shell, *hexacoordination*.<sup>13)</sup> One of the imaginary modes at a second-order saddle point is equivalent to the imaginary mode at a saddle point, and the other is a symmetric motion. The symmetric motion for copper(II) and zinc(II) follows the simultaneous leaving of two water molecules, and causes a distortion leading to *pentacoordination* where five water molecules are placed in the first shell.<sup>5a)</sup>

**Relationship between the Structural Stability and  $d$ -Electron Configuration in Heptacoordination.** As is ap-

parent from the frequency of the modes given in Tables 1 and 2, the heptahydrated divalent cations of the earlier members are located at the local minima, those of the middle members are at the saddle points, and those of the later members are at the second-order saddle points, except for the manganese(II), which is at a local minimum. A critical point is found between titanium(II) and vanadium(II) in the series, where the structural character changes from a local minimum to a saddle point; the other is seen between cobalt(II) and nickel(II), where the structural character varies from a saddle point to a second-order saddle point.

For earlier members, the hydration energies of the heptahydrated divalent cations at the saddle points become more negative than those at the local minima.<sup>5b)</sup> Similarly, the hydration energies of the heptahydrated divalent cations at the second-order saddle points are more negative than those at the saddle points (see Tables 1 and 2). The heptahydrated divalent cations with  $d^0$ ,  $d^1$ , and  $d^2$  configurations are at the local minima, the  $d^3$  and  $d^4$  cations are the saddle points, the  $d^5$  cation is at the local minimum, the  $d^6$  and  $d^7$  cations are at the saddle points, and the  $d^8$ ,  $d^9$ , and  $d^{10}$  cations are at the second-order saddle points. The structural stability of the heptacoordinated divalent cations in the first transition series is dependent on their  $d$ -electron configurations and independent of the magnitude of the hydration energy.

The three highest occupied orbitals of the water molecule are illustrated in Scheme 1. The interaction of a  $d$  orbital of the central cation with type-I or type-III orbitals is of the  $\pi$ -type. The interaction with a type-II orbital is of the  $\sigma$ -type. Scheme 2 shows an overview of the energy levels and molecular orbitals formed by the interaction between type-II

Table 1. Metal–Oxygen Bond Lengths, Electronic Properties, Hydration Energies, and Harmonic Vibrational Frequencies for Heptahydrated Divalent Cations of Earlier Members in the First Transition Series

	Ca(II) <sup>a)</sup>	Sc(II) <sup>b,c)</sup>	Ti(II) <sup>b)</sup>	V(II) <sup>b)</sup>	Cr(II)	Mn(II) <sup>b)</sup>
$d$ Configuration <sup>b)</sup>	$d^0$	$d^1$ ( $b^{(1)}$ )	$d^2$ ( $b^{(1)}$ )( $a^{(1)}$ )	$d^3$ ( $b^{(1)}$ )( $a^{(1)}$ )( $b^{(2)}$ )	$d^4$ ( $b^{(1)}$ )( $a^{(1)}$ )( $b^{(2)}$ )( $a^{(2)}$ )	$d^5$ ( $b^{(1)}$ )( $a^{(1)}$ )( $b^{(2)}$ )( $a^{(2)}$ )( $a^{(3)}$ )
Bond length <sup>e)</sup>						
M–O <sub>1</sub>	2.487	2.394	2.350	2.238	2.188	2.343
M–O <sub>2</sub>	2.511	2.418	2.350	2.235	2.795	2.384
M–O <sub>3</sub>	2.511	2.446	2.350	2.235	2.795	2.384
M–O <sub>4</sub>	2.498	2.497	2.387	2.703	2.295	2.356
M–O <sub>5</sub>	2.498	2.364	2.387	2.703	2.295	2.356
M–O <sub>6</sub>	2.454	2.339	2.321	2.220	2.137	2.264
M–O <sub>7</sub>	2.454	2.386	2.321	2.220	2.137	2.264
Total Energy <sup>f)</sup>	–1208.883791	–1291.850794	–1380.501200	–1474.955833	–1575.347848	–1681.850801
Electronic state	$^1A$	$^2A$	$^3B$	$^4A$	$^5A$	$^6A$
$\langle S^2 \rangle$ <sup>g)</sup>	0.0000	0.7505	2.0009	3.7517	6.0026	8.7517
Hydration energy <sup>h)</sup>	–262.6	–283.8	–296.3	–310.8	–308.9	–301.8
Frequency <sup>i)</sup>	29.4	31.8	35.5	128.7i	76.5i	28.6
Nature <sup>j)</sup>	Local minimum	Local minimum	Local minimum	Saddle point	Saddle point	Local minimum

a) In Ref. 5a. b) Ref. 5b. c)  $C_1$  structure. d) The orbital types in the lower column are defined in Scheme 2. The  $b^{(1)}$ -type orbital is occupied for *heptacoordination* of scandium(II) in  $C_1$  structure. e) In Å. 1 Å = 100 pm. f) In atomic unit. 1 a.u. = 2628.3 kJ mol<sup>–1</sup>. g) Total squared-magnitude of the spin. h) In kcal mol<sup>–1</sup>. 1 kcal mol = 4.1884 kJ mol<sup>–1</sup>. All the values are corrected by BSSE (basis set super-position error). The total energy of a water molecule is –76.046801 a.u. i) In cm<sup>–1</sup>. 1 cm<sup>–1</sup> = 1.98648 × 10<sup>–23</sup> J. For structures at local minima, the lowest real frequency is given. For the structures at saddle points and second-order saddle points, all the imaginary frequencies are given. j) Nature of a stationary point on the potential energy surface, i.e., local minimum, saddle point or second-order saddle point.

Table 2. Metal–Oxygen Bond Lengths, Electronic Properties, Hydration Energies, and Harmonic Vibrational Frequencies for Heptahydrated Divalent Cations of Later Members in the First Transition Series

	Fe(II)	Fe(II) <sup>a)</sup>	Co(II)	Ni(II)	Cu(II) <sup>b)</sup>	Zn(II) <sup>b)</sup>
<i>d</i> Configuration <sup>c)</sup>	$d^6$ $(b^{(1)})^2(a^{(1)})(b^{(2)})(a^{(2)})(a^{(3)})$	$d^6$ $(b^{(1)})(a^{(1)})^2(b^{(2)})(a^{(2)})(a^{(3)})$	$d^7$ $(b^{(1)})^2(a^{(1)})^2(b^{(2)})(a^{(2)})(a^{(3)})$	$d^8$ $(b^{(1)})^2(a^{(1)})^2(b^{(2)})(a^{(2)})(a^{(3)})$	$d^9$ $(b^{(1)})^2(a^{(1)})^2(b^{(2)})(a^{(2)})(a^{(3)})^2$	$d^{10}$ $(b^{(1)})^2(a^{(1)})^2(b^{(2)})^2(a^{(2)})^2(a^{(3)})^2$
Bond length <sup>e)</sup>						
M–O <sub>1</sub>	2.313	2.262	2.306	2.148	2.052	2.260
M–O <sub>2</sub>	2.321	2.323	2.262	3.133	2.292	2.261
M–O <sub>3</sub>	2.321	2.323	2.262	3.133	2.292	2.261
M–O <sub>4</sub>	2.347	2.321	2.318	2.063	2.284	2.306
M–O <sub>5</sub>	2.347	2.321	2.318	2.063	2.284	2.306
M–O <sub>6</sub>	2.197	2.243	2.176	2.090	2.274	2.152
M–O <sub>7</sub>	2.197	2.243	2.176	2.090	2.274	2.152
Total energy <sup>c)</sup>	–1794.410460	–1794.409757	–1913.341280	–2038.763874	–2170.797844	–2309.648693
Electronic state	$^5B$	$^5A$	$^4B$	$^3B$	$^2A$	$^1A$
$\langle S^2 \rangle^d)$	6.0045	6.0042	3.7536	2.0024	0.7509	0.0000
Hydration energy <sup>g)</sup>	–314.5	—	–323.6	–334.7	–328.7	–328.9
Frequency <sup>h)</sup>	100.2i	498.5i	24.6i	127.5i 110.0i	189.7i, 158.1i	126.8i 86.9i
Nature <sup>i)</sup>	Saddle point	Saddle point	Saddle point	Second-order saddle point	Second-order saddle point	Second-order saddle point

a) The structure in the state with higher energy. b) In Ref. 5a. c) The orbital types in the lower column are defined in Scheme 2. d) In Å. 1 Å = 100 pm. e) In atomic unit. 1 a.u. = 2628.3 kJ mol<sup>–1</sup>. f) Total squared-magnitude of the spin. g) In kcal mol<sup>–1</sup>, 1 kcal mol<sup>–1</sup> = 4.1884 kJ mol<sup>–1</sup>. All the values are corrected by BSSE (basis set super-position error). The total energy of a water molecule is –76.046801 a.u. h) In cm<sup>–1</sup>, 1 cm<sup>–1</sup> = 1.98648 × 10<sup>–23</sup> J. For structures at local minima, the lowest real frequency is given. For the structures at saddle points and second-order saddle points, all the imaginary frequencies are given. i) Nature of a stationary point on the potential energy surface, i.e., local minima, saddle point or second-order saddle point.

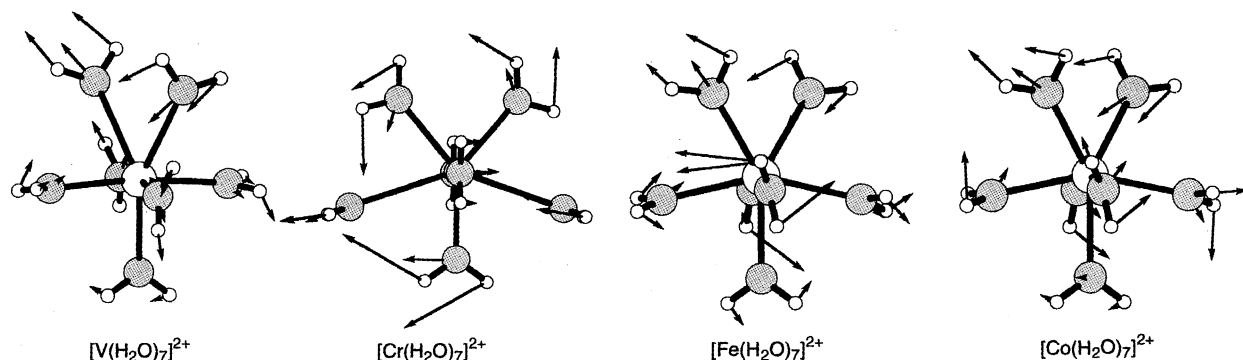
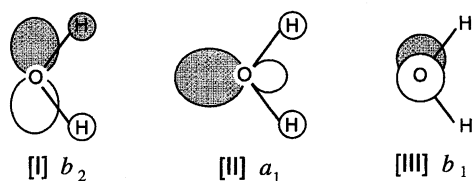
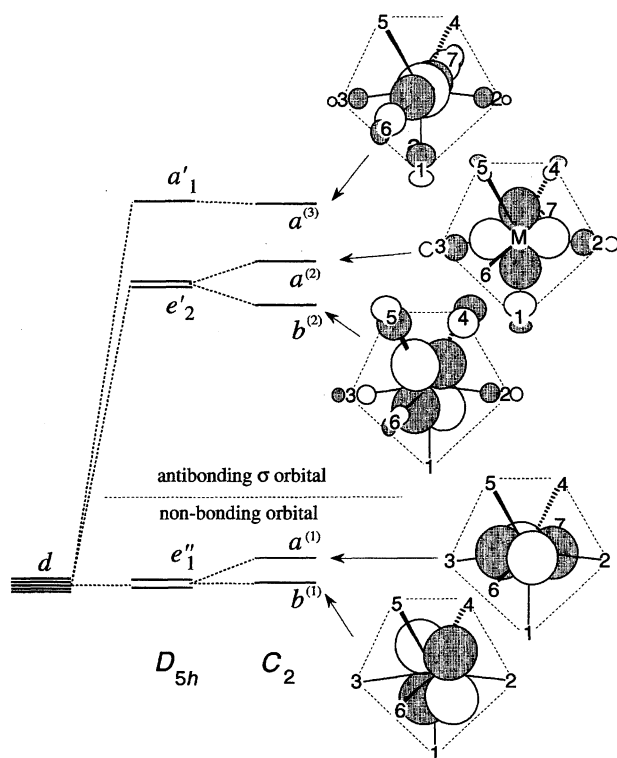


Fig. 2. Transition vectors in the concerted motion of both the entering of a water molecule toward the central cation and the leaving of a water molecule away from the central cation for heptahydrated vanadium(II), chromium(II), iron(II), and cobalt(II) ions.



Scheme 1.



Scheme 2.

orbitals of the seven water molecules and the  $d$  orbitals. In the seven-coordinated regular pentagonal-bipyramidal structure, five  $3d$  orbitals interact with the  $a_1$  orbitals of coordinating water molecules and split into two lower non-bonding orbitals ( $e'_1$ ) and three higher antibonding ones ( $e'_2$ ,  $a'_1$ ). A correlation between the orbitals in  $D_{5h}$  symmetry and the ones in the optimized  $C_2$  structures is shown in Scheme 2. The  $e'_1$  orbitals are correlated with the lowest  $a$  and  $b$  orbitals,

$e'_2$  orbitals relate to the  $a$  and  $b$  orbitals, and the  $a'_1$  orbital corresponds to the highest  $a$  orbital.

Bader–Pearson's second-order perturbation theory says that a normal mode with the same symmetry as a transition density makes the total energy of the species lower.<sup>14)</sup> There is a transition density induced by an interaction between an antibonding orbital and the empty  $4s$  orbital, which is the lowest unoccupied orbital in the heptahydrated divalent cations. The transition density due to an interaction with the antibonding  $b$  orbital ( $b \times 4s$ ) matches the antisymmetric distortion concerning the concerted motion of the entering and leaving water molecules in a water-exchange reaction. Figure 3 shows the distribution of the transition densities of the heptahydrated vanadium(II) and chromium(II) ions. The interaction between an antibonding  $a$  orbital and the empty  $4s$  orbital ( $a \times 4s$ ) produces a transition density concerning the symmetric stretching motion. The occupation of the antibonding  $d$  orbitals, through the interaction with  $4s$ , causes a distortion to a structure with a lower energy. It is possible that the *heptacoordinations* with the  $d^3$  to  $d^{10}$  configurations are located at the saddle points or higher-order saddle

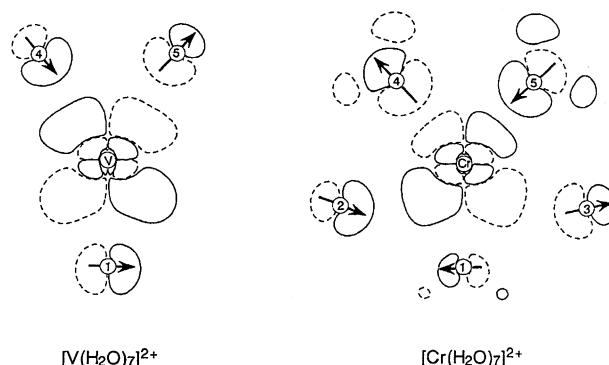


Fig. 3. Contour maps of the transition density given by a direct product of the antibonding  $b$  orbital and  $4s$  orbital ( $b \times 4s$ ) for heptahydrated vanadium(II) and chromium(II) ions. An area where the transition density has negative values is surrounded by a dotted line. An area where the transition density has positive values is surrounded by a solid line. An arrow directed from a negative area to a positive one indicates the direction of distortion.

points. Thus, the heptahydrated calcium(II), scandium(II), and titanium(II) ions are located at the local minima, and the heptahydrated divalent cations of the later members are located at the saddle or higher-order saddle point, except for this manganese(II) ion. This exception will be discussed later.

The frequency of the modes depends on the degree of bonding, which is influenced by the occupation of the antibonding orbitals, strength of the Coulombic interaction, and the degree of mixing between a  $d$  orbital of the central cation and the orbitals of the ligands.

The change in the structural stability between cobalt(II) and nickel(II) in the series is largely affected by the degree of bonding. The distortion, corresponding to the transition density resulting from the occupation of antibonding  $a$  orbitals, gives rise to a simultaneous elimination of two water molecules. This distortion is energetically unfavorable for the ions of the earlier members, which retain the bonding character, because none of the antibonding  $d$  orbitals of these ions are doubly occupied. Therefore, the *heptacoordinations* of the ions from chromium(II) to cobalt(II) in the series are not located at the higher-order saddle points. This distortion turns favorable for the *heptacoordination* of nickel(II) ion, which has two long bonds (Ni–O<sub>2</sub> and Ni–O<sub>3</sub>) without a bonding character due to the doubly occupied antibonding  $a$  orbital. The heptahydrated copper(II) and zinc(II) ions are also located at the second-order saddle point due to the same reason.

The *heptacoordinations* of the ions from vanadium(II) to cobalt(II) in the series are located at saddle points, except for that of manganese(II). The large Coulombic interaction and degree of mixing of the orbitals make the heptahydrated manganese(II) ion to be located at a local minimum. Figure 4 shows the natural atomic charge<sup>15)</sup> on the central cation and the distribution of antibonding  $b$  orbitals of the *heptacoordinations* of the ions from vanadium(II) to cobalt(II) in the series. The atomic charge, both the natural atomic charge and Mulliken charge, on the central cation is larger for the

later members than the earlier ones, while the manganese(II) has the largest atomic charge. Stabilization by a Coulombic interaction is the largest for the manganese(II). The distribution of the antibonding  $b$  orbitals in Fig. 4 suggests that the orbital coefficients of the  $d$  orbital in the antibonding orbitals decrease across the periodic table row from left to right. The largest stabilization is expected when the orbital coefficients of a  $d$  orbital and water-molecules are equal to each other. Because two electrons occupy the bonding  $b$  orbital and one electron occupies the antibonding  $b$  orbital, the bonds corresponding to the orbitals are stabilized by an electron. The orbital mixing is largest for the heptahydrated manganese(II) ion, where the extent of the  $d$  orbital is as large as those of ligands.

An associative process for activation is operative in the water exchange on a hexahydrated ion when the *heptacoordination* of the ion is located at a local minimum or a saddle point on the potential surface.<sup>5a)</sup> The associative mechanism should be operative for water-exchange reactions on hexahydrated divalent cations with a  $d$  configuration less than seven.

**Cis and Trans Attack.** It has been discussed how the entering ligand stereochemically attacks during ligand substitution reactions of hexacoordinate complexes.<sup>16)</sup> The possible reaction schemes and related transition states with transition vectors are shown in Scheme 3. The transition states for water exchange have the entering (X) and leaving (Y) water molecules in the *cis* or *trans* position to each other by a *cis* attack or a *trans* attack, respectively. The transition density and the strength of bonding at *heptacoordination* decide where the actual displacement occurs, i.e., the *cis* or *trans* position. They are dependent on the amplitude of the orbital coefficient based on the type-II orbital (Scheme 1) of the water molecules in the antibonding  $b$  orbital.

*Heptacoordinations* with one or more occupied antibonding  $d$  orbitals are divided into two groups. One involves those with  $d^3$ ,  $d^5$ ,  $d^6$ ,  $d^7$ ,  $d^9$ , and  $d^{10}$  configurations which have a distorted equatorial plane; the other involves those

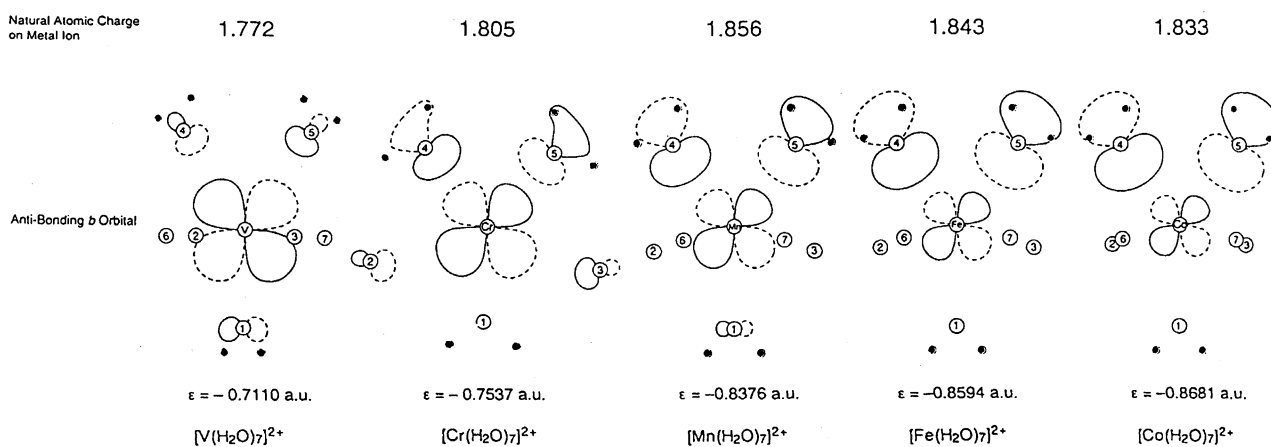
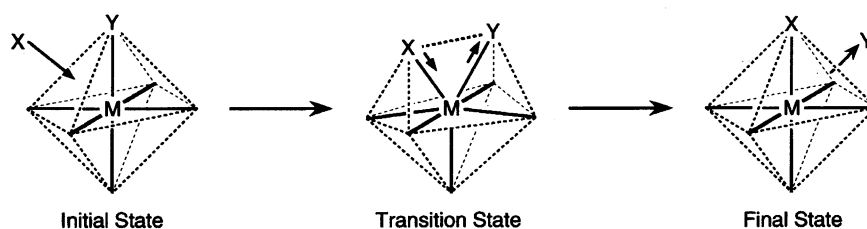
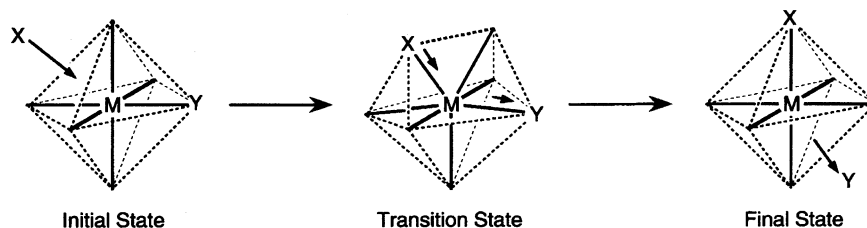


Fig. 4. Natural atomic charges of the central cations and contour maps of the antibonding  $b$  orbitals of heptahydrated vanadium(II), chromium(II), manganese(II), iron(II), and cobalt(II) ions on the plane defined by the 4 and 5 oxygen atoms and the central cation. The numbering of oxygen atoms is shown in Fig. 1. Dots refer to hydrogen atoms and numbered circles show oxygen atoms projected into the plane.  $\epsilon$  is the UHF orbital energy in atomic unit (1 a.u. = 2628.3 kJ mol<sup>-1</sup>).

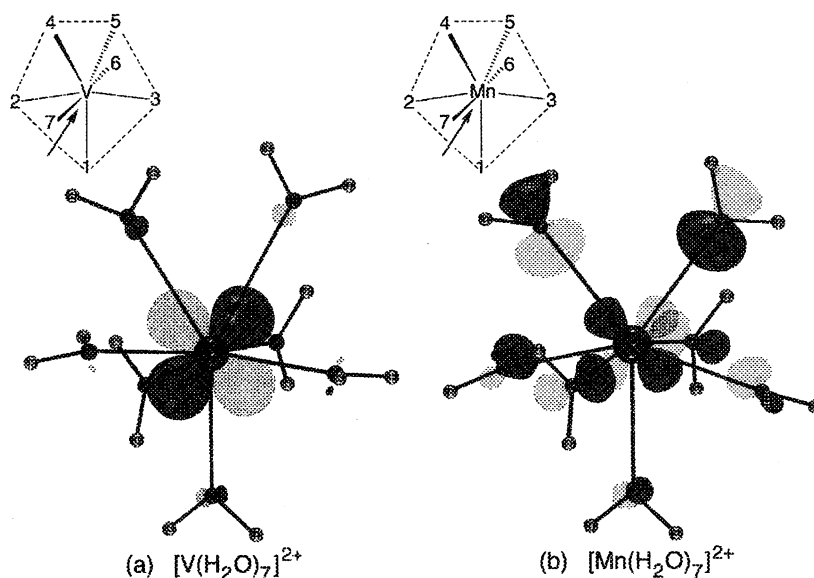
*cis* attack*trans* attack

Scheme 3.

with  $d^4$  and  $d^8$  configurations of the  $^3B$  state, which has a flat equatorial plane. The occupancy of the antibonding  $a$  orbitals determines the pattern of the antibonding interaction. In the following discussion we use the numbering of water molecules as shown in Fig. 1. The *heptacoordinations* are also classified as to the type of antibonding  $b$  orbital. One is the *heptacoordination* with a  $d^3$  configuration where the orbital coefficients of water molecules exist only on the 4 and 5 water molecules (Fig. 5a). The others have significant orbital coefficients on the 2 and 3 water molecules as well as on the 4 and 5 water molecules. Figure 5b shows this type  $b$  orbital of heptahydrated manganese(II) ion. In all cases, the orbital coefficients of the 4 and 5 water molecules are larger than those of the 2 and 3 water molecules in the antibonding  $b$  orbital. Therefore, a *cis* attack is preferred for all of these

*heptacoordinations* if only the transition density selects the method of attack. Actually, these are large transition vectors at the 4 and 5 water molecules in the *heptacoordinations* with the  $d^3$ ,  $d^6$ ,  $d^7$ ,  $d^9$ , and  $d^{10}$  configurations (vanadium(II), iron(II), cobalt(II), copper(II), and zinc(II)). All of these *heptacoordinations* have a distorted equatorial plane. In the case of the  $d^3$  vanadium(II), the large antibonding interaction with the 4 and 5 also enhances displacement of the water molecules. On the other hand, these is a large transition vector in the *trans* position in the case of  $d^4$  chromium(II). The occupation of one of the antibonding  $a$  orbitals enhances the antibonding interaction with the 2 and 3 water molecules, and reduces the antibonding interaction with the 4 and 5 water molecules which move to the nodal plane of the  $d$  orbital.

The antisymmetric imaginary vibration of heptahydrated

Fig. 5. 3-D distributions of antibonding  $b$  orbitals of heptahydrated vanadium(II) (a) and manganese(II) (b) ions.

nickel(II) ion in the  $^3B$  state has a large *trans* vibrational mode, which is similar to the imaginary mode of the heptahydrated chromium(II) ion, while those of copper(II) and zinc(II) have a large *cis* vibration mode.

The water-exchange reaction on hexahydrated divalent cations from  $d^3$  vanadium(II) to  $d^7$  cobalt(II) in the series, on which an associative process for activation is operative, prefers *cis* attack. On the other hand, the water exchange prefers *trans* attack when the pentagonal bipyramidal *heptacoordination* has a flat equatorial plane. In the case of the operative associative process of the water-exchange reaction, the hexahydrated divalent cations with  $d^3$ ,  $d^6$ , and  $d^7$  configurations prefer a *cis* attack, while the  $d^4$  cation prefers a *trans* attack due to the structure dependency of *heptacoordination* on the occupancy of the antibonding *a* orbitals.

### Conclusions

We studied the stability of the heptahydrated divalent cations as model intermediary species on associative reaction pathways for all members of the first transition series in order to clarify the change in the mechanism of the water-exchange reaction on the hexahydrated divalent cations in water as the central elements are changed.

1. All of the structures of *heptacoordination* obtained in this study are pentagonal bipyramidal with a distorted equatorial plane, except for  $d^4$  and  $d^8$  cations with the flat equatorial plane. The structural stability of the heptacoordinated divalent cations in the first transition series is dependent on their *d* electron configuration; the heptahydrated divalent cations with  $d^0$ ,  $d^1$ , and  $d^2$  configurations are located at the local minima, those with  $d^3$  and  $d^4$  configurations are at the saddle points, the  $d^5$  cation is at the local minimum, the  $d^6$  and  $d^7$  cations are at the saddle points, and the  $d^8$ ,  $d^9$ , and  $d^{10}$  cations are at the second-order saddle points. The associative mechanism is operative for water exchange on hexahydrated divalent cations with less than seven *d* electrons, because the seven-coordinate cations regarded as an intermediary species are located at the local minima or at the saddle points on the potential-energy surface.

2. The occupation of the antibonding *d* orbitals determines the structural stability of the *heptacoordination*. The transition density related to the antibonding *b* orbital and unoccupied 4s orbital causes an energy lowering with an antisymmetric distortion.

3. The occupancy of the antibonding *a* orbital determines the pattern of the antibonding interaction of *heptacoordination*. In the operative associative process of the water-exchange reaction, the hexahydrated divalent cations with  $d^3$ ,  $d^6$ , and  $d^7$  configurations prefer a *cis* attack, while those with a  $d^4$  configuration prefer a *trans* attack.

This work was partially supported by a Grant-in-Aid for Scientific Research Nos. 09740423 and 09874131 from the Ministry of Education, Science, Sports and Culture.

### References

- 1) C. N. Langford and H. B. Gray, "Ligand Substitution Processes," Benjamin Inc., New York (1966).
- 2) H. Ohtaki and T. Radnai, *Chem. Rev.*, **93**, 1157 (1993).
- 3) a) A. E. Merbach, *Pure Appl. Chem.*, **59**, 161 (1987); b) R. van Eldik, T. Asano, and W. J. le Noble, *Chem. Rev.*, **89**, 549 (1989).
- 4) a) R. Åkesson, L. G. M. Pettersson, M. Sandström, P. E. M. Siegbahn, and U. Wahlgren, *J. Phys. Chem.*, **97**, 3765 (1993); b) R. Åkesson, L. G. M. Pettersson, M. Sandström, and U. Wahlgren, *J. Am. Chem. Soc.*, **116**, 8705 (1994); c) S.-K. Kang, B. Lam, T. A. Albright, and J. F. O'Brien, *New J. Chem.*, **15**, 757 (1991).
- 5) a) Y. Tsutsui, H. Wasada, and S. Funahashi, *Bull. Chem. Soc. Jpn.*, **70**, 1813 (1997); b) Y. Tsutsui, H. Wasada, and S. Funahashi, *Bull. Chem. Soc. Jpn.*, **71**, 73 (1998).
- 6) a) F. P. Rotzinger, *J. Am. Chem. Soc.*, **118**, 6760 (1996); b) F. P. Rotzinger, *J. Am. Chem. Soc.*, **119**, 5230 (1997); c) M. Hartmann, T. Clark, and R. van Eldik, *J. Am. Chem. Soc.*, **119**, 7843 (1997).
- 7) A. J. H. Wachters, *J. Chem. Phys.*, **52**, 1033 (1970).
- 8) a) S. Huzinaga, *J. Chem. Phys.*, **42**, 1293 (1965); b) T. H. Dunning, *J. Chem. Phys.*, **53**, 2823 (1970).
- 9) a) R. Åkesson, L. G. M. Pettersson, M. Sandström, and U. Wahlgren, *J. Phys. Chem.*, **96**, 10773 (1992); b) R. Åkesson, L. G. M. Pettersson, M. Sandström, and U. Wahlgren, *J. Am. Chem. Soc.*, **116**, 8691 (1994).
- 10) S. F. Boys and F. Bernardi, *Mol. Phys.*, **19**, 553 (1970).
- 11) a) M. J. Frisch, G. W. Trucks, M. Head-Gordon, P. M. W. Gill, M. W. Wong, J. B. Foresman, B. G. Johnson, H. B. Schlegel, M. A. Robb, E. S. Replogle, R. Gomperts, J. L. Andres, K. Raghavachari, J. S. Binkley, C. Gonzalez, R. L. Martin, D. J. Fox, D. J. Defrees, J. Baker, J. J. P. Stewart, and J. A. Pople, "Gaussian 92, Revision C," Gaussian Inc., Pittsburgh, PA (1992); b) M. J. Frisch, G. W. Trucks, H. B. Schlegel, P. M. W. Gill, B. G. Johnson, M. A. Robb, J. R. Cheeseman, T. Keith, G. A. Petersson, J. A. Montgomery, K. Raghavachari, M. A. Al-Laham, V. G. Zakrzewski, J. V. Ortiz, J. B. Foresman, J. Cioslowski, B. B. Stefanov, A. Nanayakkara, M. Challacombe, C. Y. Peng, P. Y. Ayala, W. Chen, M. W. Wong, J. L. Andres, E. S. Replogle, R. Gomperts, R. L. Martin, D. J. Fox, J. S. Binkley, D. J. Defrees, J. Baker, J. P. Stewart, M. Head-Gordon, C. Gonzalez, and J. A. Pople, "Gaussian 94, Revision C.3," Gaussian Inc., Pittsburgh, PA (1995).
- 12) a) Y. Tsutsui and H. Wasada, *Chem. Lett.*, **1995**, 517; b) H. Wasada and Y. Tsutsui, *Bull. Fac. General Educ., Gifu University*, **33**, 145 (1996).
- 13) We pursued a reaction pathway of the water-exchange reaction on the hexahydrated vanadium(II) ion, in which the  $I_a$  mechanism was experimentally accepted. The intrinsic reaction path leading down from the *heptacoordination* to the *hexacoordination* (hexaaqua vanadium(II) ion with a water molecule in the second coordination shell) showed that the *heptacoordination* is the transition state of the water-exchange reaction on the vanadium(II) ion. Furthermore, we evaluated the relation between the low imaginary frequency for the *heptacoordination* of cobalt(II) and the reaction path of the water-exchange reaction. The geometry optimization was performed with computing second derivatives of the potential surface. The atomic coordinates at the starting point were those of the *heptacoordination* slightly moved along the transition vector in proportion to its amplitude. The distance between the central cobalt atom and the leaving water molecule increased monotonously and

the structure changed to the *hexacoordination*. These findings indicate that the *heptacoordination* is the transition state of the water-exchange reactions via the associative mechanism.

14) R. F. W. Bader, *Can. J. Chem.*, **40**, 1164 (1962).

15) A. E. Reed, R. B. Weinstock, and F. Weinhold, *J. Chem. Phys.*, **83**, 1164 (1985).

16) F. Basolo and R. G. Pearson, "Mechanisms of Inorganic Chemistry," 2nd ed, John Wiley & Sons, Inc., New York (1967).

---